Fast 3D Optical Mammography using ICG Dynamics for Reader Independent Lesion Differentiation

S. Piper[1], P. Schneider[2], N. Volkwein[2], N. Schreiter[2], C. H. Schmitz[1,3],A. Poellinger[2]
[1]*Charité, Department of Neurology, Charitéplatz 1, 10117 Berlin, Germany*
[2]*Charité, Department of Radiology, Augustenburger Platz 1, 13353 Berlin, Germany*
[3]*NIRx Medizintechnik GmbH, Baumbachstr. 17, 13189 Berlin, Germany*
Sophie.Piper@charite.de

Abstract: Based on ICG bolus kinetics of the absorption changes in the reconstructed DOT images in suspicious lesion bearing breasts, we derived a reader independent classification between malignant and benign lesions with high sensitivity and specificity.
OCIS codes: (170.6960) Tomography; (170.3830) Mammography; (170.6935) Tissue characterization

1. Introduction

We conducted a contrast-enhanced optical mammography study using ICG as an unspecific blood pool agent and demonstrated the benefit of high-frame rate absorption tomography [1]. With a temporal resolution of about 0.5 sec 3D perfusion data can be derived that are feasible for feature-based classification or self-organized segmentation approaches as known from perfusion imaging in fMRI or dynamic CT, PET or SPECT[2,3] in various clinical applications as cerebral ischemia or myocardium perfusion for example.

Previously reported absorption measurements were able to study some aspects of the breast's ICG pharmacokinetics [4]; however, to our knowledge none of these have been performed at scan rates that adequately sample the early bolus dynamics in the tissue. In this report we describe a reader independent analysis approach to automatically differentiate malignant from benign lesions due to non-invasively measured early ICG bolus kinetics. We are the first to derive an automated classification algorithm based on perfusion parameters measured with DOT. This numerical approach focuses on temporal information of ICG perfusion in the whole breast without demanding any a priori information on the spatial distribution of lesions.

2. Methods

Optical Mammography scans were carried out with a DYNOT 232 optical tomography system (NIRx Medical Technologies LLC, NY, USA) customized for mammography studies as described in detail in [5]. Subjects were lying in prone position on a modified patient bed with an opening and an adjustable gantry below holding a rigid plastic cup with 31 co-located source and detector fibers. Varying the protrusion of the fibers into the cup allowed accommodation to different breast sizes and assured good contact between the breast tissue and fiber sensors. The imager performs sequential illumination with 760 nm and 830 nm at each fiber position while simultaneously acquiring detector readings for each illumination site, resulting in a total of 961 measurements at a rate of approx. 2 Hz. Total recording time was over 2000 frames corresponding to about 20 minutes. Following an initial 5 min resting phase, a single bolus of 25 mg ICG (Pulsion AG, Munich, Germany) dissolved in 15 ml aqua ad injectionem was injected (injection time: 5 s), followed by a 15 ml saline solution.

The study was approved by the hospital's ethics committee and all patients gave written informed consent. We recruited 22 patients of the radiology clinics who had high probability for breast occupying lesions and who were scheduled for needle biopsy. Overall 14 breasts bearing a malignant lesion and eight breasts bearing a benign lesion were analyzed.

Data were preprocessed and reconstructed using the MATLAB (The Mathworks, Inc., Natick, MA) based NIRx NAVI software (Near Infrared Analysis, Visualization and Imaging, Rev. 8.11 by NIRx). Data were first low-pass filtered (f_{cutoff} ~0.075 Hz) and then normalized to the temporal mean value during the initial resting phase. Channels exhibiting too much noise (coefficient of variation > 25%) during the rest phase were excluded. The automated reconstruction of 3D time series of relative ICG concentration changes over a total of 2243 volume segments covering the entire breast cup utilized the normalized-difference as described in [6].

Further data analysis was performed using customized routines in Matlab. From each image time series the bolus peak amplitude (PA - maximum amplitude for each time course normalized to the maximum of the mean amplitude of the entire breast volume) and the time to peak (TTP) were determined. To rule out differences in overall blood circulation between subjects the reference time point (t_0) for the TTP was not set to bolus administration or onset, but to the earliest point in time when more than 0.25% of the breast volume has already had

its bolus peak. Furthermore, a third parameter was defined that we called 'peak time grouped amplitude' (PTA). Here, for each time point x following t_0 the mean peak amplitude over all volume segments simultaneously exhibiting its maximum at the time t_0 + x was calculated. The median over all benign and malignant cases respectively was visualized in a PA-vs.-TTP curve (PTA curve) from which the time point x=1.5 sec was chosen to be the most distinguishable point in time between both groups as calculated by the maximum standardized mean difference (SMD). The PTA distributions between the malignant and the benign group at time point t_0 + 1.5 sec were tested with a Wilcoxon rank sum test for equal medians. From these distributions, a cut-off value of 84.4,% was derived to categorize each breast in malignant, if its PTA value at the time point t_0 + 1.5 sec was above 84.4% of the maximum mean breast intensity and in benign if below that threshold. Sensitivity and specificity were calculated for this threshold.

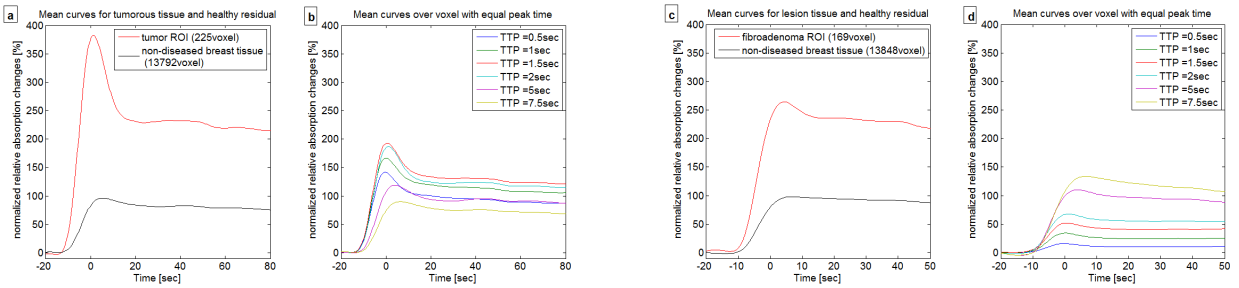

Figure 1. Reconstructed absorption changes for two representative subjects (a+b: 53y, 33mm invasive ductal carcinoma; c+d: 22y, 22mm firboadenoma). Subplot a and c show the mean time courses over the lesion (red) and over the residual non-diseased tissue (black), respectively, each normalized to the maximum of the mean amplitude of the entire breast volume. Subplot b and d show normalized mean time courses over all volume segments with equal time to peak in the respective subject. Reference time point (t=0) was set to the appearance of first bolus peaks in the breast.

3. Results

Fig. 1 shows typical results of the reconstructed concentration changes for a malignant (a+b) and a benign (c+d) lesion, respectively. Typical time courses are displayed for a region of interest over the lesion sight (as confirmed by MRI or ultrasound and palpation), for the spatially averaged response over all residual (predominantly un-diseased) volume segments as well as for different peak times the normalized mean time courses over all volume segments having an equal time to peak.

A prominent initial bolus peak (starting around t_0, duration ~10-15 sec) occurs only in a fraction of the imaged volume and not in the average response. The distribution of mean time courses for different peak times vary between the malignant and the benign case.

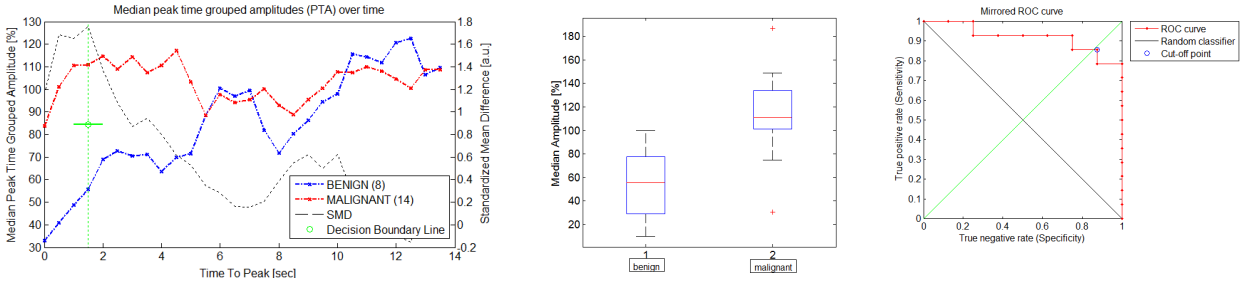

Figure 2. Left: Median peak time grouped amplitudes (PTA) over increasing time to peak for malignant (blue) and benign (red) group, respectively. The decision boundary line of the classification is illustrated in green. Middle: Boxplot of the amplitude distribution over all voxel with a TTP of t_0 + 1,5 sec and all malignant and benign patients respectively. Right: Mirrored ROC curve for peak amplitudes with a TTP of t_0 + 1,5 sec. The decision boundary line for highest sensitivity an specificity in our data set is 84.4%.)

Figs. 2 presents the reader independent classification approach. On the left the PA-vs.-TTP curve of the median over all benign and malignant cases respectively is shown from which the time point x=1.5 sec was chosen to be the most distinguishable point in time between both groups as calculated by the maximum SMD and proven significant by a Wilcoxon rank sum test for equal medians (p=0.0015, middle column). The right column shows the corresponding mirrored ROC curve giving us a cut_off PTA value of 84.4% at time point x=1.5 sec that leads to highest sensitivity and specificity results in our dataset with 85.7% and 87.5% respectively.

Table 1 summarizes all cases imaged and the detection rates for benign and malignant lesions. Furthermore the lesion localization, while illustrating the areas of high and early PTA values, was in good agreement with other imaging modalities such as MRI or classical mammography (data not shown here).

Table 1. Summary of study results.

Malignant, mean lesion size (range)	**Detection Rate**	**Benign, mean lesion size (range)**	**Detection Rate**
Invasive ductal carcinoma , 29mm (8-51mm)	8 / 9	Fibro-cystic mastopathy, 11mm	0 / 1
Invasive lobular carcinoma, 25mm	1 / 1	Fibroadenoma, 24mm (10-51mm)	1 / 6
Invasive lobular ductal carcinoma, 17mm	0/1	Pseudoangiomatous stromalhyperplasia (PASH), 44mm	0 / 1
Metaplastic carcinoma, 28mm (19-37mm)	2 / 2		
Ductal carcinoma in situ, 80mm	1 / 1		
Sum	**12 / 14**	**Sum**	**1 / 8**

4. Conclusions

Measuring early ICG enhancement following bolus injection with a high-frame rate optical imaging device allows a reader-independent differentiation between malignant and benign breast lesions. The algorithm is very promising and might serve as an adjunct method to x-ray mammography. To further investigate the robustness of the suggested approach more patient data would be desirable.

5. References

[1] P. Schneider, S. Piper,C.H. Schmitz, N.F. Schreiter, N. Volkwein,L. Lüdeman, U. Malzahn, A.Poellinger, " Fast 3D Near-Infrared Breast Imaging Using Indocyanine Green for Detection and Characterization of Breast Lesions," Rofo,183(10):956-63(2011).

[2] S. Oeltze, H. Doleisch , H. Hauser, P. Muigg,B. Preim B, "Interactive visual analysis of perfusion data",Nov-Dec;13(6):1392-9(2007).

[3] A. Wismueller, O. Lange, "Cluster Analysis of Biomedical Image Time-Series", International Journal of Computer Vision 46(2): 103–128, (2002)

[4] B. Alacam, B. Yazici, X. Intes, S. Nioka, and B. Chance, "Pharmacokinetic-rate images of indocyanine green for breast tumors using near-infrared optical methods," Phys. Med. Biol. 53, 837-859 (2008).

[5] C.H. Schmitz, D.P. Klemer, R.E. Hardin, M.S. Katz, Y. Pei, H.L. Graber, M.B. Levin, R.D. Levina, N.A. Franco, W.B. Solomon, and R.L. Barbour, "Design and implementation of dynamic near-infrared optical tomographic imaging instrumentation for simultaneous dual-breast measurements," Applied Optics, Vol. 44, pp. 2140-2153 (2005).

[6] R.L. Barbour, H.L. Graber, Y. Pei, S. Zhong, and C.H. Schmitz, "Optical tomographic imaging of dynamic features of dense-scattering media," J. Optical Society of America A, Vol. 18, pp. 3018-3036 (2001).